

Exploring salinity origins in the Ghiss-Nekor aquifer, northern Morocco: a multivariate statistical analysis

Abdelhak Bourjila^{1*}, *Fouad Dimane*¹, *Mohammad Ghalit*², *Morad Taher*³, *Salim Kamari*⁴, *Yahya El Hammoudani*¹, *Iliass Achoukhi*¹, *Hatim Faiz*¹, *Khadija Haboubi*¹, and *Lahcen Benaabidate*⁵

¹Laboratory of Engineering Sciences and Applications (LSIA)- Materials Science, Energy and Environment (SM2E) Research team, ENSAH / Abdelmalek Essaâdi University, Al Hoceima, Morocco

²Laboratory of Research and Development in Engineering Sciences, Faculty of Sciences and Techniques of Al-Hoceima (FSTH), Abdelmalek Essaâdi University, Tetouan, Morocco

³ Department of Geology, Applied Geosciences and Geological Engineering Research Team, FSTH, Abdelmalek Essaâdi University, Al Hoceima, Morocco

⁴ Environmental Management and Civil Engineering Research Team, Laboratory of Applied Sciences, ENSAH, Abdelmalek Essaâdi University, Al Hoceima, Morocco

⁵ Department of Environment, Laboratory of Functional Ecology and Environment Engineering, Faculty of Sciences and Techniques, University Sidi Mohamed Ben Abdellah, Fez, Morocco

Abstract. The Ghiss-Nekor coastal aquifer is characterized by high salinity stemming from multiple sources, remains poorly investigated. This study aims to address this knowledge gap by employing both univariate (descriptive statistics) and multivariate statistical analyses, including correlation matrix and principal component analysis (PCA). Groundwater samples were collected from 52 sites across the study area and meticulously analyzed for pH, TDS, EC, and the ions such as Na⁺, K⁺, Mg²⁺, Ca²⁺, NH₄⁺, HCO₃⁻, NO₃⁻, NO₂⁻, Cl⁻, SO₄²⁻, PO₄³⁻, and SiO₂. Descriptive statistics, notably standard deviation (SD), highlight the diverse sources contributing to salinization, among which seawater intrusion (SWI) emerges as a significant factor. Correlation matrix analysis underscores multiple pathways for salinization, implicating SWI, salt dissolution, chemical weathering, secondary salt leaching, and anthropogenic activities. PCA elucidates 81.05% of the total variance in physicochemical parameters, with strong loadings observed for EC, Na⁺, Cl⁻, and Mg²⁺, corroborating the influence of SWI and suggesting evaporation processes. Moreover, PCA reinforces the potential influence of both geogenic and anthropogenic factors in salinization within the study area. This comprehensive investigation provides valuable insights into the elevated salinity levels observed in the Ghiss-Nekor aquifer, contributing to a deeper understanding of its hydrogeochemical dynamics.

* Corresponding author: abourjila@uae.ac.ma

1 Introduction

Groundwater salinization has emerged as a global environmental concern, exerting significant impacts on countries worldwide. It incurs substantial ecological and economic costs while posing a threat to global health [1], and is widely recognized as a major form of water pollution [2]. Managing and governing groundwater effectively proves challenging, particularly in arid and semi-arid environments [3, 4]. Therefore, it is crucial to identify the sources of groundwater salinization and comprehend the underlying processes and mechanisms, especially in coastal aquifers due to their complex nature and diverse sources.

One of the effective multivariate statistical methods is the Principal Component Analysis (PCA), which plays a pivotal role in identifying sources of salinity in aquifers. By condensing numerous physicochemical parameters of groundwater into key factors, this method facilitates understanding of the aquifer characteristics and behavior regarding salinization and other water pollution sources [5, 6].

The Ghiss-Nekor aquifer serves as the primary groundwater storage in the Al-Hoceima province, a semi-arid Mediterranean area plagued by elevated groundwater salinity. This issue complicates drinking water supply management, worsened by reduced regulation capacity of the principal dam in the area (MBAK dam) as a result of silt accumulation [7]. Understanding the origins of salinization in this area is pivotal for managing the region's drinking water resources effectively.

Several studies have assessed the physico-chemical quality of groundwater in the Ghiss-Nekor plain, including those by [8], [9], [10], [11], [12], [13], [14], [15], and [16]. This study aims to complement these efforts by employing both univariate and multivariate statistical analyses to discern potential sources of salinization in the Ghiss-Nekor aquifer, by using the descriptive statistics, correlation matrix, and principal component analysis (PCA). This approach, emerging as an indispensable tool for informing water management strategies, aims to unravel the intricacies of groundwater salinity origins.

2 Study area

The Ghiss-Nekor plain (Fig. 1) lies southeastern Al-Hoceima in Northern Morocco. The area is intersected by the Ghiss River, which flows through the northwest, and the Nekor River, which traverses its center. Beneath the plain lies the Ghiss-Nekor aquifer, regarded as a principal alluvial aquifer in Morocco's Mediterranean region, spanning approximately 90 km². Estimates suggest the aquifer holds total reserves of around 328 million cubic meters (MCM) [17]. Geographically, the plain is delimited by the Imzouren-fault (NNW-SSE) to the West and the Trougout-fault (N-S) to the East; these faults are characterized as normal faults with a strike-slip component [18]. Geological formations within the aquifer (Fig. 2) extend from depths of 200 to 450 meters and mainly comprise coarse sand and gravel, with occasional mixtures of clay and silt, along with sporadic clay-marly lenses. Additionally, there is a wide clayey layer that extends prominently along the coast. Beneath the aquifer lies a bedrock composed of impermeable shale substratum. The region experiences a semi-arid Mediterranean climate, marked by gentle, rainy winters and scorching, arid summers. Rainfall typically occurs from October to April, while the dry, hot season extends from May to September. On average, the study area experiences a yearly temperature of 18°C, with intermittent yearly rainfall averaging 346mm [19].

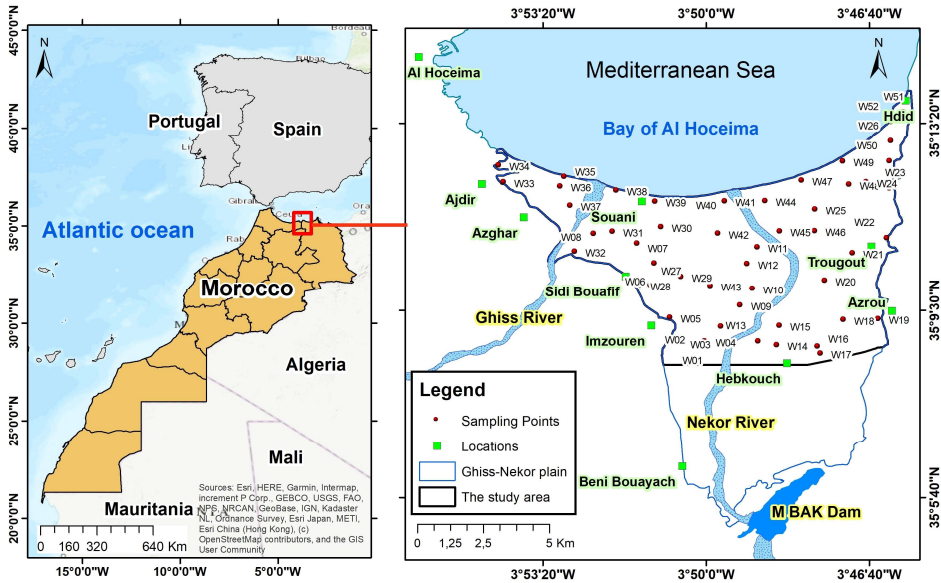


Fig. 1. The study area location.

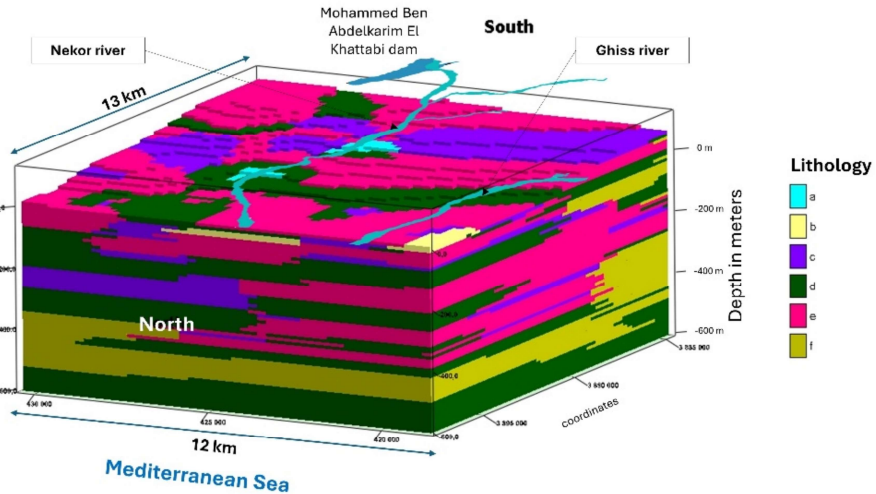


Fig. 2. Lithologic model of the Ghiss-Nekor aquifer. Lithology: (a) Abundance of gravel and pebble, (b) Abundance of shell sand, (c) Alluvial deposit with silt and clay, (d) Clay, marl, and silt, (e) Coarse sand and gravel, (f) Shale.

3 Materials and methods

In January 2022, groundwater sampling was conducted in accordance with the guidelines set forth in the 9th edition of "Water analysis" [20], including storage, transportation, and laboratory analysis procedures. The parameters T (temperature), pH (acidity or alkalinity), and EC (electrical conductivity) were measured using the Multifunction pH Meter PCE-PHD-1. Total dissolved solids (TDS) were determined by summing the levels of cations and

anions present in the water samples. Sodium (Na^+) and potassium (K^+) levels were determined using ELICO Digital Flame Photometer CL- 378 with an accuracy of ± 0.5 ppm. Calcium (Ca^{2+}) and magnesium (Mg^{2+}) concentrations were analyzed via titration with EDTA. Chloride ions (Cl^-) were measured through titration with silver nitrate (0.1 N), while bicarbonate ions (HCO_3^-) were determined using titration with hydrochloric acid (0.1 N). Nitrate (NO_3^-), nitrite (NO_2^-), ammonium (NH_4^+), phosphate (PO_4^{3-}), sulfate (SO_4^{2-}), and silica (SiO_2) levels were quantified using a colorimetric determination method with a Hach Lange DR 6000 UV-VIS Spectrophotometer, with a precision of ± 1 nm. The univariate and the multivariate statistics were conducted using SPSS 25.0 software. These methods are commonly used and beneficial for examining large datasets to comprehend geochemical assessments and pinpoint potential geological factors affecting groundwater chemistry.

4 Results and discussion

4.1 Descriptive statistics

Table 1 presents a summary of the essential data regarding the physicochemical properties of the Ghiss-Nekor groundwater. The pH levels range from 7.1 to 8.2, indicating an alkaline nature, with an average of 7.6. It is notable that the pH exhibits a very low standard deviation (0.3), suggesting a consistent source across samples [21]. The EC ranges from 1612 to 15300 $\mu\text{S}/\text{cm}$, averaging 4076.3 $\mu\text{S}/\text{cm}$, while the TDS vary from 1449.5 to 10014.8 mg/L, with an average of 3043.6 mg/L. Cation abundance follows the sequence: $\text{Na}^+ > \text{Ca}^{2+} > \text{Mg}^{2+} > \text{K}^+ > \text{NH}_4^+$, whereas anions follow: $\text{SO}_4^{2-} > \text{Cl}^- > \text{HCO}_3^- > \text{NO}_3^- > \text{PO}_4^{3-} > \text{NO}_2^-$. This order of abundance aligns with findings by [22] upstream of the Ghiss-Nekor plain.

The variability in measured concentrations of hydrochemical parameters, as indicated by their standard deviations, is substantial, with notable observed disparities, particularly in Cl^- (823.6 mg/L), which ranges from 156 to 5140.7 mg/L, and averages 858.6 mg/L. These fluctuations imply the presence of multiple potential sources of salinization within the study area [23]. Seawater intrusion is identified as a potential contributor to salinization, evident from significant fluctuations (SD) in EC (2337.8 $\mu\text{S}/\text{cm}$) and TDS (1520.2 mg/L) [21].

Table 1. Descriptive statistics of the measured groundwater parameters.

| Parameter | | Mean | Median | Minimum | Maximum | Std. deviation |
|--------------------|-----------------------------|--------|--------|---------|---------|----------------|
| pH | - | 7.6 | 7.6 | 7.1 | 8.2 | 0.3 |
| EC | ($\mu\text{S}/\text{cm}$) | 4076.3 | 3480.0 | 1612.0 | 15300.0 | 2337.8 |
| TDS | | 3043.6 | 2717.5 | 1449.5 | 10014.8 | 1520.2 |
| Na^+ | | 529.6 | 436.0 | 137.0 | 2560.0 | 413.8 |
| K^+ | | 7.2 | 4.3 | 1.7 | 40.4 | 7.7 |
| Mg^{2+} | | 142.7 | 131.0 | 56.6 | 395.5 | 65.6 |
| Ca^{2+} | | 226.9 | 223.6 | 59.3 | 415.2 | 74.5 |
| NH_4^+ | | 0.0187 | 0.0141 | 0.000 | 0.182 | 0.0294 |
| Cl^- | mg/L | 858.6 | 627.5 | 156.0 | 5140.7 | 823.6 |
| SO_4^{2-} | | 873.1 | 857.4 | 235.1 | 1592.2 | 312.6 |
| HCO_3^- | | 377.8 | 359.9 | 152.5 | 713.7 | 104.1 |
| NO_3^- | | 29.526 | 19.790 | <DL* | 123.360 | 26.681 |
| NO_2^- | | 26.379 | 0.000 | <DL* | 1371.0 | 190.122 |
| PO_4^{3-} | | 0.0795 | 0.0422 | <DL* | 0.5413 | 0.1109 |
| SiO_2 | | 20.5 | 15.3 | 5.5 | 81.0 | 16.6 |

* DL : Detection limit. The DL for NO_3^- , NO_2^- , and NH_4^+ are 0.01 mg/L, 0.03 mg/L, and 0.002 mg/L, respectively.

4.2 Correlation analysis of hydrochemical parameters

The correlation matrix was employed to evaluate the extent of association among different groundwater parameters, as outlined in Table 2. A robust association between these parameters is indicated by coefficients of +1 or -1, while 0 signifies no connection. Values falling between +0.50 to +0.70 suggest moderate correlation, those between +0.70 and +0.90 indicate high correlation, and coefficients at +0.90 or above signify very high correlation. These three correlation coefficient categories were highlighted in bold within the correlation matrix. The significant positive associations of (Na^+ , Cl^- , Mg^{2+} , and K^+) with (EC and TDS) underscore that these major ions predominantly govern the observed high salinity, likely originating from common sources [21], such as seawater intrusion occurrence [24] and salt dissolution [4, 25]. The exceptionally strong correlation between Na^+ and Cl^- (+0.99) underscores the influences of chemical weathering, secondary salt leaching, and seawater intrusion [26–28]. Likewise, the strong correlation between Ca^{2+} and SO_4^{2-} (+0.92) indicates a possible shared origin, such as gypsum ($\text{CaSO}_4 \cdot 2\text{H}_2\text{O}$) or anhydrite (CaSO_4) dissolution [4, 28, 29]. However, the substantial correlations of Mg^{2+} with Ca^{2+} (+0.74), Na^+ (+0.84), and Cl^- (+0.85) highly suggest common origins, chiefly seawater intrusion and carbonate dissolution [28]. The significant correlations between K^+ and Na^+ , as well as Cl^- , imply a shared source, particularly near the shoreline where these ions are abundant, suggesting that seawater infiltration could be a potential factor contributing to salinity increase in coastal areas [25]. SiO_2 demonstrates a high correlation with PO_4^{3-} (+0.95) and moderate correlations with NO_3^- (+0.60), with SiO_2 being geogenic while PO_4^{3-} and NO_3^- are predominantly anthropogenic, originating from sources like septic systems, manure, and commercial fertilizers [30]. The strong correlation between SiO_2 , PO_4^{3-} , and NO_3^- can be attributed to enhanced silicate weathering due to the nitrification process [31]. Weak to very weak correlations between NH_4^+ , NO_3^- , NO_2^- , PO_4^{3-} with most variables (EC, TDS, Na^+ , K^+ , Mg^{2+} , Ca^{2+} , Cl^-) indicate diverse sources for these ions, suggesting human activities such as sewage leaks and agricultural practices have influenced groundwater chemistry. The presence of a highly insignificant negative correlation ($-0.37 < r < 0.32$) observed between pH and the other parameters suggests minimal impact of pH fluctuations on groundwater salinity [25].

Table 2. Matrix of correlations of the measured parameters.

| Ions | Na^+ | K^+ | Mg^{2+} | Ca^{2+} | NH_4^+ | Cl^- | SO_4^{2-} | HCO_3^- | NO_3^- | NO_2^- | PO_4^{3-} | SiO_2 | EC | TDS | pH |
|--------------------|---------------|--------------|------------------|------------------|-----------------|---------------|--------------------|------------------|-----------------|-----------------|--------------------|----------------|------------|------|----|
| Na^+ | 1 | | | | | | | | | | | | | | |
| K^+ | .79 | 1 | | | | | | | | | | | | | |
| Mg^{2+} | .84 | .56 | 1 | | | | | | | | | | | | |
| Ca^{2+} | .49 | .20 | .74 | 1 | | | | | | | | | | | |
| NH_4^+ | .14 | .24 | .23 | .18 | 1 | | | | | | | | | | |
| Cl^- | .99 | .77 | .85 | .50 | .16 | 1 | | | | | | | | | |
| SO_4^{2-} | .38 | .14 | .69 | .92 | .20 | .36 | 1 | | | | | | | | |
| HCO_3^- | .19 | .02 | .26 | -.01 | -.09 | .14 | .02 | 1 | | | | | | | |
| NO_3^- | .21 | .18 | .04 | -.15 | .03 | .19 | -.16 | .12 | 1 | | | | | | |
| NO_2^- | .26 | .17 | .11 | -.14 | -.05 | .24 | -.12 | .19 | .33 | 1 | | | | | |
| PO_4^{3-} | .18 | .25 | -.06 | -.29 | -.03 | .16 | -.36 | .16 | .61 | .03 | 1 | | | | |
| SiO_2 | .18 | .22 | -.08 | -.26 | -.04 | .16 | -.37 | .14 | .60 | .05 | .95 | 1 | | | |
| EC | .99 | .75 | .91 | .60 | .18 | .99 | .49 | .19 | .15 | .15 | .12 | .12 | 1 | | |
| TDS | .97 | .71 | .93 | .68 | .18 | .96 | .58 | .21 | .15 | .15 | .07 | .07 | .99 | 1 | |
| pH | -.22 | -.04 | -.18 | -.26 | .32 | -.19 | -.18 | -.37 | -.03 | .05 | -.18 | -.23 | -.22 | -.25 | 1 |

4.3 Principal component analysis (PCA)

PCA analysis was employed to explore the underlying sources of variation in hydrochemical variables, condensing a multitude of individual parameters into a more concise set while preserving their inherent attributes [23]. This approach aids in spotlighting the primary

variables impacting groundwater chemistry. In this study, PCA was executed through orthogonal varimax rotation alongside Kaiser normalization, a frequently employed rotation method known to mitigate the influence of less significant groundwater quality parameters identified through PCA analysis [32]. The analysis focused on 13 chosen variables representing the geochemical framework. To assess the dataset's suitability for PCA, Kaiser Meyer Olkin (KMO) and Bartlett's tests [33] were conducted, with the results detailed in Table 3. A KMO value exceeding 0.5 and a Bartlett's test significance below 0.05 reflecting significant correlation within the data. In this investigation, the KMO sufficiency value stood at 0.642, with a significance value of less than 0.001.

Four principal components (Eigenvalues >1) were selected, collectively explaining 81.05% of the total variance. Component 1 accounted for 40.12%, component 2 for 23.21%, component 3 for 9.60%, and component 4 for 8.12%. Table 4 presents the respective loadings for each component, with loadings exceeding 0.65 highlighted. These were employed to examine the connections between components and hydrochemical parameters [23].

Component 1, termed the "salinization component," displays strong positive loadings for EC, Na⁺, Cl⁻, Mg²⁺ with values of +0.98, +0.94, +0.96, and +0.92, respectively, and moderately positive loadings for K⁺, Ca²⁺, and SO₄²⁻ with values of +0.78, +0.63, and +0.54, respectively, suggesting potential influence from seawater intrusion. Component 2 showcases robust positive-loadings for PO₄³⁻ (+0.91), SiO₂ (+0.90), and NO₃⁻ (+0.67), indicative of anthropogenic sources such as domestic sewage and agricultural run-off [31]. Component 3 is characterized by a strong positive loading of NO₂⁻, pointing to pollution from human activities, particularly evident in urban areas such as Imzouren [9, 33]. Component 4 displays a moderately positive loading of NH₄⁺, likely attributed to agricultural practices or sewage seepage [35], while HCO₃⁻ exhibits a negative correlation, indicative of natural processes like carbonate mineral dissolution [36].

These PCA findings highlight complex hydrogeochemical processes, including weathering of recharge area material, evaporation, seawater intrusion, and anthropogenic influences such as agriculture and residential sewage seepage.

Table 3. Kaiser–Meyer–Olkin (KMO) test and Bartlett’s test of sphericity.

| Tests | Measured value |
|---|-----------------------|
| Kaiser-Meyer-Olkin (KMO) Measure of sampling sufficiency | .64 |
| Approximate Chi-Square value | 987.71 |
| Bartlett's test of sphericity | |
| df | 78 |
| Sig. | <0.001 |

df: degrees of freedom; Sig. : significance

Table 4. Rotated matrix of components for the measured parameters.

| Parameters | Component | | | |
|-------------------------------|------------|------------|------------|------------|
| | 1 | 2 | 3 | 4 |
| EC | .98 | .02 | .09 | -.02 |
| Na ⁺ | .97 | .12 | .04 | -.04 |
| Cl ⁻ | .96 | .10 | .04 | .00 |
| Mg ²⁺ | .92 | -.24 | .13 | -.06 |
| K ⁺ | .78 | .29 | -.15 | .19 |
| Ca ²⁺ | .63 | -.56 | .28 | .10 |
| PO ₄ ³⁻ | .13 | .91 | .07 | -.05 |
| SiO ₂ | .12 | .90 | .10 | -.05 |
| NO ₃ ⁻ | .13 | .67 | .57 | .03 |
| SO ₄ ²⁻ | .54 | -.64 | .26 | .10 |
| NO ₂ ⁻ | .05 | .05 | .87 | -.08 |
| HCO ₃ ⁻ | .22 | .10 | -.03 | -.78 |
| NH ₄ ⁺ | .25 | -.02 | -.10 | .68 |
| Eigenvalue | 5.22 | 3.02 | 1.25 | 1.06 |
| Variance (%) | 40.12 | 23.21 | 9.60 | 8.12 |
| Cumulative (%) | 40.12 | 63.33 | 72.93 | 81.05 |

The highlighted values indicate positive-loadings of the associated parameters within the extracted components.

5 Conclusion

The study provides a comprehensive understanding of the elevated salinity levels observed in the Ghiss-Nekor aquifer, shedding light on the hydrogeochemical dynamics and underlying sources of salinization in the region. Through a combination of descriptive statistics, correlation matrix analysis, and principal component analysis (PCA), the study elucidates the complex interplay of various factors contributing to groundwater salinity. The findings reveal significant correlations among physicochemical parameters, emphasizing the dominant influence of seawater intrusion, salt dissolution, chemical weathering, secondary salt leaching, and anthropogenic activities. PCA analysis further consolidates these insights, identifying distinct components associated with salinization, anthropogenic contamination, and specific pollutants originating from human activities such as agriculture and urban sewage. Moreover, the study highlights the multifaceted nature of hydrogeochemical processes within the Ghiss-Nekor aquifer, including weathering of recharge area materials, evaporation, and the intricate interplay between geogenic and anthropogenic influences. These insights are crucial for formulating effective water management strategies aimed at mitigating salinity issues and preserving the quality of groundwater resources in the region.

We extend our sincere gratitude to the reviewers for their valuable feedback, which substantially improved the quality of this manuscript.

References

1. C. Li, X. Gao, S. Li, and J. Bundschuh, A review of the distribution, sources, genesis, and environmental concerns of salinity in groundwater. *Environ. Sci. Pollut. Res.* **27**, 41157–41174. (2020). <https://doi.org/10.1007/s11356-020-10354-6>.
2. W.D. Williams, Salinization of Rivers and Streams: An Important Environmental Hazard. *Ambio.* **16**, 180–185. (1987).
3. M. Taher, T. Mourabit, I. Etebaai, H.C. Dekkaki, N. Amarjouf, A. Amine, B. Abdelhak, A. Errahmouni, and S. Azzouzi, Identification of Groundwater Potential Zones (GWPZ) Using Geospatial Techniques and AHP Method: a Case Study of the Boudinar Basin,

- Rif Belt (Morocco). *Geomat. Environ. Eng.* **17**, 83–105. (2023).
<https://doi.org/10.7494/geom.2023.17.3.83>.
4. B. Askri, A.T. Ahmed, and R. Bouhlila, Origins and processes of groundwater salinisation in Barka coastal aquifer, Sultanate of Oman. *Phys. Chem. Earth. (Pt A/B/C)*. **126**, 103116. (2022). <https://doi.org/10.1016/j.pce.2022.103116>.
 5. M.A.A. Mohammed, N.P. Szabó, and P. Szűcs, Multivariate statistical and hydrochemical approaches for evaluation of groundwater quality in north Bahri city-Sudan. *Heliyon*. **8**, e11308. (2022). <https://doi.org/10.1016/j.heliyon.2022.e11308>.
 6. X. Lu, Y. Fan, Y. Hu, H. Zhang, Y. Wei, and Z. Yan, Spatial distribution characteristics and source analysis of shallow groundwater pollution in typical areas of Yangtze River Delta. *Sci. Total Environ.* **906**, 167369. (2024).
<https://doi.org/10.1016/j.scitotenv.2023.167369>.
 7. M. Taher, T. Mourabit, A. Bourjila, O. Saadi, A. Errahmouni, F.E. Marzkioui, and M.E. Mousaoui, An Estimation of Soil Erosion Rate Hot Spots by Integrated USLE and GIS Methods: a Case Study of the Ghiss Dam and Basin in Northeastern Morocco. *Geomat. Environ. Eng.* **16**, 95–110. (2022). <https://doi.org/10.7494/geom.2022.16.2.95>.
 8. A. Bourjila, F. Dimane, M. Ghalit, M. Taher, S. Kamari, Y. El Hammoudani, I. Achoukhi, and K. Haboubi, Mapping the spatiotemporal evolution of seawater intrusion in the Moroccan coastal aquifer of Ghiss-Nekor using GIS-based modeling. *Water Cycle*. **4**, 104–119. (2023). <https://doi.org/10.1016/j.watcyc.2023.05.002>.
 9. S. Kamari, H.E. Ouarghi, M. Ghalit, A. Makan, and A. Bourjila, Risk of Groundwater Contamination by Domestic Wastewater in Rural Areas of the Province of Al Hoceima, Northern Morocco. *Ecol. Eng. Environ. Technol.* **24**. (2023).
 10. Y.E. Hammoudani, F. Dimane, K. Haboubi, A. Bourjila, C. Benaissa, I. Achoukhi, and C. Haboubi, Assessment of groundwater quality in the lower wadi of the Nekor valley, Al-Hoceima-Morocco. *Environ. Eng. Manag. J.* **22**, 399–409. (2023).
<https://doi.org/10.30638/eemj.2023.031>.
 11. D. Chafouq, A. El Mandour, M. Elgettafi, M. Himi, I. Chouikri, and A. Casas, Hydrochemical and isotopic characterization of groundwater in the Ghis-Nekor plain (northern Morocco). *J. Afr. Earth. Sci.* **139**, 1–13. (2018).
<https://doi.org/10.1016/j.jafrearsci.2017.11.007>.
 12. N. Nouayti, E.K. Cherif, M. Algarra, M.L. Pola, S. Fernández, A. Nouayti, J.C.G. Esteves da Silva, K. Driss, N. Samlani, H. Mohamed, et al., Determination of Physicochemical Water Quality of the Ghis-Nekor Aquifer (Al Hoceima, Morocco) Using Hydrochemistry, Multiple Isotopic Tracers, and the Geographical Information System (GIS). *Water*. **14**, 606. (2022). <https://doi.org/10.3390/w14040606>.
 13. S. Benyoussef, H. El Ouarghi, and Y. El Yousfi, Qualitative assessment of the waters of the coastal aquifer Ghis-Nekor (Central Rif, Northern Morocco) in view of agricultural use. *J. Water Land Dev.* **52**, 245–250. (2022).
<https://doi.org/10.24425/jwld.2022.140395>.
 14. A. Salhi, Géophysique, hydrogéologie et cartographie de la vulnérabilité et du risque de pollution de l'aquifère de Ghis-Nekor (Al Hoceima, Maroc), Ph.D. thesis, Abdelmalek Essaâdi University, Faculty of Sciences, Tetouan (2008).
 15. C. Benaissa, B. Bouhmadi, and A. Rossi, An assessment of the physicochemical, bacteriological quality of groundwater and the water quality index (WQI) used GIS in Ghis Nekor, Northern Morocco. *Sci. Afr.* **20**, e01623. (2023).
<https://doi.org/10.1016/j.sciaf.2023.e01623>.

16. S. Bouhout, C. Haboubi, K. Haboubi, M.S. Elyoubi, A. Elabdouni, M.E. Bastrioui, and H.E. Alaoui, Spatial variability of nitrate leaching and risk assessment of nitrate contamination in the Ghiss-Nekor alluvial aquifer system (Northeastern Morocco) through Disjunctive Kriging. *Sci. Afr.* **23**, e02009. (2024). <https://doi.org/10.1016/j.sciaf.2023.e02009>.
17. ONEE, L'étude de l'adduction d'eau brute de la station de traitement d'Al Hoceima à partir du barrage projeté sur l'Oued Ghiss (Office National de l'électricité et de l'Eau potable-Branche Eau, Direction Technique et Ingénierie (DTI)) (2017).
18. M. Taher, T. Mourabit, A. Errahmouni, and A. Bourjila, New Tectonic and Topometric Evidence of Modern Transtensional Tectonics in the Low Nekor Basin (NE Morocco). In *Proceedings of MedGU 2021, Istanbul* (2023). https://doi.org/10.1007/978-3-031-43222-4_38.
19. S. Bouhout, K. Haboubi, A. Zian, M.S. Elyoubi, and A. Elabdouni, Evaluation of two linear kriging methods for piezometric levels interpolation and a framework for upgrading groundwater level monitoring network in Ghiss-Nekor plain, north-eastern Morocco. *Arab. J. Geosci.* **15**, 1016. (2022). <https://doi.org/10.1007/s12517-022-10283-3>.
20. J. Rodier, B. Legube, N. Merlet, and R. Brunet, *L'analyse de l'eau - 9ème édition - Eaux naturelles, eaux résiduaires, eau de mer: Eaux naturelles, eaux résiduaires, eau de mer 9ème édition.* (Dunod, 2009).
21. N.U. Kura, M.F. Ramli, S. Ibrahim, W.N.A. Sulaiman, and A.Z. Aris, An integrated assessment of seawater intrusion in a small tropical island using geophysical, geochemical, and geostatistical techniques. *Environ. Sci. Pollut. Res.* **21**, 7047–7064. (2014). <https://doi.org/10.1007/s11356-014-2598-0>.
22. M. Ghalit, E.B. Yousfi, M. Zouhairi, E.K. Gharibi, and J.-D. Taupin, Hydrochemical characterization of groundwater in the Nekor basin located in the North-East of the Rif of Morocco. *Mor. J. Chem.* **5**, 5-2 (2017) 272-284. (2017).
23. Md.M.R. Sarker, M. Van Camp, D. Hossain, M. Islam, N. Ahmed, Md.M. Karim, Md.A.Q. Bhuiyan, Md.A. Ahsan, and K. Walraevens, Hydrochemical characterization and groundwater potential of the deep aquifer system in southwest coastal region of Bangladesh. *J. Asian Earth Sci.* **234**, 105271. (2022). <https://doi.org/10.1016/j.jseaes.2022.105271>.
24. Y. Kim, K.-S. Lee, D.-C. Koh, D.-H. Lee, S.-G. Lee, W.-B. Park, G.-W. Koh, and N.-C. Woo, Hydrogeochemical and isotopic evidence of groundwater salinization in a coastal aquifer: a case study in Jeju volcanic island, Korea. *J. Hydrol.* **270**, 282–294. (2003). [https://doi.org/10.1016/S0022-1694\(02\)00307-4](https://doi.org/10.1016/S0022-1694(02)00307-4).
25. A. Gebeyehu, T. Ayenew, and A. Asrat, Hydrogeochemistry of the groundwater system of the transboundary basement and volcanic aquifers of the Bulal catchment, Southern Ethiopia. *J. Afr. Earth Sci.* **194**, 104622. (2022). <https://doi.org/10.1016/j.jafrearsci.2022.104622>.
26. M.V. Prasanna, S. Chidambaram, A. Shahul Hameed, and K. Srinivasamoorthy, Study of evaluation of groundwater in Gadilam basin using hydrogeochemical and isotope data. *Environ. Monit. Assess.* **168**, 63–90. (2010). <https://doi.org/10.1007/s10661-009-1092-5>.
27. K. Srinivasamoorthy, C. Nanthakumar, M. Vasanthavigar, K. Vijayaraghavan, R. Rajivgandhi, S. Chidambaram, P. Anandhan, R. Manivannan, and S. Vasudevan, Groundwater quality assessment from a hard rock terrain, Salem district of Tamilnadu, India. *Arab. J. Geosci.* **4**, 91–102. (2011). <https://doi.org/10.1007/s12517-009-0076-7>.

28. M.F. Abu Al Naeem, I. Yusoff, T.F. Ng, J.P. Maity, Y. Alias, R. May, and H. Alborsh, A study on the impact of anthropogenic and geogenic factors on groundwater salinization and seawater intrusion in Gaza coastal aquifer, Palestine: An integrated multi-techniques approach. *J. Afr. Earth Sci.* **156**, 75–93. (2019).
<https://doi.org/10.1016/j.jafrearsci.2019.05.006>.
29. D. Dobrzyński, Chemical diversity of groundwater in the Carboniferous-Permian aquifer in the Unisław Śląski - Sokółowsko area (the Sudetes, Poland); a geochemical modelling approach. *Acta Geol. Pol.* **57**, 97–112. (2007).
30. N. Ağca, S. Karanlık, and B. Ödemiş, Assessment of ammonium, nitrate, phosphate, and heavy metal pollution in groundwater from Amik Plain, southern Turkey. *Environ. Monit. Assess.* **186**, 5921–5934. (2014). <https://doi.org/10.1007/s10661-014-3829-z>.
31. B. Batsaikhan, S.-T. Yun, K.-H. Kim, S. Yu, K.-J. Lee, Y.-J. Lee, and J. Namjil, Groundwater contamination assessment in Ulaanbaatar City, Mongolia with combined use of hydrochemical, environmental isotopic, and statistical approaches. *Sci. Total Environ.* **765**, 142790. (2021). <https://doi.org/10.1016/j.scitotenv.2020.142790>.
32. I. Said, and S.A. Salman, Salinization of groundwater under desert reclamation stress at Qena region, Egypt. *J. Afr. Earth Sci.* **181**, 104250. (2021).
<https://doi.org/10.1016/j.jafrearsci.2021.104250>.
33. N. Shrestha, Factor Analysis as a Tool for Survey Analysis. **9**, 4–11. (2021).
<https://doi.org/10.12691/ajams-9-1-2>.
34. F. Mchiouer, A.A. Boughrous, and H.E. Ouarghi, Groundwater Quality Assessment for Human Drinking in Rural Areas, Al-Hoceima Province (Northern Morocco). *Ecol. Eng. Environ. Technol.* **23**, 138–147. (2022). <https://doi.org/10.12912/27197050/147450>.
35. H. Wang, Q. Yang, and J. Liang, Interpreting the salinization and hydrogeochemical characteristics of groundwater in Dongshan Island, China. *Mar. Pollut. Bull.* **178**, 113634. (2022). <https://doi.org/10.1016/j.marpolbul.2022.113634>.
36. G.O. Badmus, O.D. Akinyemi, A.M. Gbadebo, and J.A. Oyedepo, Hydrochemical analysis of groundwater quality along the coastal aquifers in part of Ogun Waterside, Ogun State, southwestern Nigeria. *Heliyon.* **6**, e05661. (2020).
<https://doi.org/10.1016/j.heliyon.2020.e05661>.